



EUROfusion

WPEDU-CPR(18) 20147

A Tsimpoukis et al.

**Rarefied pulsatile pressure-driven fully
developed gas flow in long circular
tubes**

Preprint of Paper to be submitted for publication in Proceeding of
9th GRACM 2018 International Congress on Computational
Mechanics



This work has been carried out within the framework of the EUROfusion Consortium and has received funding from the Euratom research and training programme 2014-2018 under grant agreement No 633053. The views and opinions expressed herein do not necessarily reflect those of the European Commission.

This document is intended for publication in the open literature. It is made available on the clear understanding that it may not be further circulated and extracts or references may not be published prior to publication of the original when applicable, or without the consent of the Publications Officer, EUROfusion Programme Management Unit, Culham Science Centre, Abingdon, Oxon, OX14 3DB, UK or e-mail Publications.Officer@euro-fusion.org

Enquiries about Copyright and reproduction should be addressed to the Publications Officer, EUROfusion Programme Management Unit, Culham Science Centre, Abingdon, Oxon, OX14 3DB, UK or e-mail Publications.Officer@euro-fusion.org

The contents of this preprint and all other EUROfusion Preprints, Reports and Conference Papers are available to view online free at <http://www.euro-fusionscipub.org>. This site has full search facilities and e-mail alert options. In the JET specific papers the diagrams contained within the PDFs on this site are hyperlinked

RAREFIED PULSATILE PRESSURE-DRIVEN FULLY-DEVELOPED GAS FLOW IN LONG CIRCULAR TUBES

Alexandros Tsimpoukis and Dimitris Valougeorgis

Laboratory of Transport Phenomena, Department of Mechanical Engineering
University of Thessaly
Volos, 38334, Greece
e-mail: atsimpoukis@mie.uth.gr; e-mail: diva@mie.uth.gr

Keywords: Pulsatile flows, Oscillatory flows, Knudsen number, BGK, Richardson effect.

Abstract. *The pulsatile pressure driven fully-developed flow of a rarefied gas through a long circular tube is investigated, based on the time-dependent linear BGK equation, by decomposing the flow into its steady and oscillatory parts. As the oscillation frequency is increased the amplitude of all macroscopic quantities is decreased, while their phase lag with respect to the pressure gradient is increased reaching the limiting value of 90° . As the gas becomes more rarefied higher frequencies are needed to trigger this behavior. The computation of the inertia and viscous forces in terms of the gas rarefaction and oscillation parameters, clarifies when the flow consists of only one oscillating viscous region or of two regions, namely the inviscid piston flow in the core and the oscillating Stokes layer at the wall with the velocity overshooting. The maximum value of the time average oscillatory pumping power is one half of the corresponding steady one.*

1 INTRODUCTION

Time-dependent vacuum gas flows are strongly related to gas distribution systems of fusion reactors, consisting of channels with different lengths and cross sections. The flow in such pipe networks varies from the free molecular regime up to the hydrodynamic limit or in the whole range of the Knudsen number. Depending on the vacuum pumping system, the driving pumps and the operating conditions, phenomena related to oscillatory gas flow may produce enhanced counter flow of gas [1,2]. The detailed investigation of the pulsatile and oscillatory motion of gases in the whole range of the Knudsen number is important to avoid such harmful phenomena and to compute the associated energy losses.

In the hydrodynamic (or viscous) regime, pulsatile and oscillatory pressure-driven fully-developed flows, through channels of various cross sections have received, over the years, considerable attention [3-6]. In the slip, transition and free molecular regimes however, where in addition to the oscillation frequency, the level of gas rarefaction plays a significant role in the flow properties and patterns, the corresponding work in rarefied pulsatile gas flows is very limited. In the slip regime, the oscillatory flow in rectangular channels has been solved in [7], based on the unsteady Stokes equation subject to slip boundary conditions. Of course, continuum-based models are valid provided that both the mean free path and time are much smaller than the characteristic channel size and the pressure gradient oscillation time respectively. Therefore, in the transition and free molecular regimes the flow must be modeled by kinetic theory based on the Boltzmann equation or reliable kinetic model equations [8].

In this framework, very recently, the rarefied oscillatory flow in a cylindrical tube has been simulated, based on the linearized BGK equation, with the assumption of small oscillatory pressure gradient amplitude [9]. Here, the analysis is extended to pulsatile flows in circular tubes and computational results are provided for the flow rate, the wall shear stress and the pumping power as well as for the acting inertia and viscous forces.

2 FLOW CONFIGURATION AND DEFINITION OF MACROSCOPIC QUANTITIES

Consider the time-dependent isothermal flow of a monatomic rarefied gas through an infinite long circular tube of radius R . The flow is caused by a pulsatile pressure gradient that consists of a constant part that does not vary in time and that produces a steady flow forward, plus an oscillatory part, with the oscillation frequency ω , that moves the fluid back and forth and that produces zero net flow over each cycle [9].

The main flow quantities of the pulsatile flow are introduced first in dimensional and then, in dimensionless form. The local pulsatile pressure gradient depends on the flow direction z' and time t' . It may be written as

$$\frac{d\hat{P}_{PUL}(t',z')}{dz'} = \frac{dP_S(z')}{dz'} + \frac{d\hat{P}(z',t')}{dz'} = \frac{dP_S(z')}{dz'} + \frac{dP(z')}{dz'} \cos(\alpha t') = \frac{dP_S(z')}{dz'} + \frac{dP(z')}{dz'} \Re[\exp(-i\alpha t')] \quad (1)$$

where $d\hat{P}_{PUL}/dz'$, dP_S/dz' and $d\hat{P}/dz'$ refer to the pulsatile, steady and oscillatory pressure gradients, $dP(z')/dz'$ is the amplitude of the oscillating pressure gradient, while \Re denotes the real part of a complex expression, with $i = \sqrt{-1}$. It is evident that the time average over one period of the pressure gradient of the oscillatory flow is zero, while of the pulsatile flow is different than zero and equal to the steady pressure gradient. Due to the linearity of Eq. (1), the steady and oscillatory parts of the pulsatile fully-developed flow can be solved independently of each other. This is a useful breakdown, because the steady part of the flow has already been solved in [8] and therefore, only the oscillatory part remains for investigation.

The pulsatile pressure gradient generates a gas flow in the z' -direction, which is characterized by its pulsatile velocity and shear stress distributions given by

$$\hat{U}_{PUL}(t',r') = U_S(r') + \hat{U}(t',r') = U_S(r') + \Re[U(r')\exp(-i\alpha t')] \quad (2)$$

$$\hat{\Pi}_{PUL}(t',r') = \Pi_S(r') + \hat{\Pi}(t',r') = \Pi_S(r') + \Re[\Pi(r')\exp(-i\alpha t')], \quad (3)$$

respectively. The superscript $\hat{}$ always denotes time-dependent quantities. The complex functions $U(r')$ and $\Pi(r')$ completely determine the oscillatory pressure driven flow. Integrating the velocity over the cross section the mean velocity and wall shear stress are defined:

$$\bar{U}_{PUL}(t') = \frac{1}{A'} \iint_{A'} \hat{U}_{PUL}(t',r') dA' = \bar{U}_S + \bar{U}(t') = \bar{U}_S + \Re[\bar{U}\exp(-i\alpha t')] \quad (4)$$

$$\hat{\Pi}_{PUL,W}(t') = \int_{\Gamma} \hat{\Pi}_{PUL}(t',r') d\Gamma' = \Pi_{S,W} + \hat{\Pi}_W(t') = \Pi_{S,W} + \Re[\Pi_W \exp(-i\alpha t')] \quad (5)$$

The quantities with the subscript ‘‘S’’ always denote the steady part, while \bar{U} and Π_W are complex and related to the oscillatory part.

Furthermore, the pulsatile mass flow rate is defined as

$$\hat{M}_{PUL}(t') = \iint_{A'} \rho(t',z') \hat{U}_{PUL}(t',r') dA' = \dot{M}_S + \dot{M}(t') = \dot{M}_S + \Re[\dot{M}\exp(-i\alpha t')] \quad (6)$$

where \dot{M}_S and $\dot{M}(t')$ denote the steady and oscillatory mass flow rates, while the mass density $\rho = \rho(t',z')$ varies in time and in the axial direction (it is constant at each cross section) and it is defined by the equation of state once the operating pressure and temperature are specified.

Next, based on the mean velocity and wall shear stress, the inertia (or acceleration) $\hat{F}'_I(t')$ and viscous $\hat{F}'_V(t')$ forces acting on a fluid volume $A'dz'$ passing through the channel are given by

$$\hat{F}'_{PUL,I}(t') = \rho dz' A' \frac{\partial \bar{U}_{PUL}(t')}{\partial t'} = \rho dz' A' \frac{\partial \bar{U}(t')}{\partial t'} = \hat{F}'_I(t') \quad (7)$$

and

$$\hat{F}'_{PUL,V}(t') = F'_{S,V} + \hat{F}'_V(t') = dz' \Gamma' (\Pi_{S,W} + \hat{\Pi}_W(t')). \quad (8)$$

As expected the inertia force is related only to the oscillatory part, while the viscous force has both steady and oscillatory parts. At any point in time, the driving pressure force

$$\hat{F}'_{PUL,P}(t') = F'_{S,P} + \hat{F}'_P(t') = A'dP_S + A'd\hat{P}(t') \quad (9)$$

must equal the net sum of the viscous and inertia forces that may add or subtract from each other at different times within the oscillatory cycle. Then, the following steady and oscillatory force balances are formed:

$$\text{Steady: } A'dP_S = dz'\Gamma'\Pi_{S,W} \quad (10)$$

$$\text{Oscillatory: } A'd\hat{P}(t') = \rho dz'A' \frac{\partial \bar{U}(t')}{\partial t'} + dz'\Gamma'\hat{\Pi}_W(t') \quad (11)$$

It is noted that due to the fully-developed flow there is no net momentum flux.

Finally, the pumping power needed to drive the pulsatile flow is defined as $\hat{E}'_{PUL}(t') = E'_S + \hat{E}'(t')$, where the steady the oscillatory pumping powers are given by the product of the corresponding acting pressure forces times the mean velocities written as $E'_S = A'dP_S\bar{U}_S$ and

$$\hat{E}'(t') = A'd\hat{P}(t')\bar{U}(t') = A'dP \cos(\alpha t') \Re[\bar{U} \exp(-i\alpha t')] \quad (12)$$

respectively. Since the oscillatory part $\hat{E}'(t')$ does not produce any net flow forward and since the steady part E'_S is the same as that in steady flow, any power expenditure on the oscillatory part of the flow reduces the efficiency of the flow. It is noted that the integral of the oscillatory pumping power over one cycle is nonzero, hence oscillatory flow requires energy to maintain even the net flow is zero.

The parameters which define the problem in dimensional form include the gas properties, the operating pressure and temperature, the channel geometry and the oscillation frequency. They are significantly reduced by introducing the corresponding quantities in dimensionless form, allowing in parallel, a more detailed flow investigation.

The two dimensionless flow parameters defining the present pulsatile flow are specified [9]. The first one is the gas rarefaction parameter δ and it is given by $\delta = \frac{PR}{\mu\nu}$, where μ is the gas viscosity at some reference temperature T and $\nu = \sqrt{2R_g T}$ is the most probable molecular speed (R_g is the gas constant). The rarefaction parameter is proportional to the inverse Knudsen number. The second one is the frequency parameter θ and it is given by $\theta = \frac{P}{\mu\omega}$, where (P/μ) is the intermolecular collision frequency and ω the oscillation frequency. Hence, small and large values of θ correspond to high and low pressure gradient oscillation respectively. As $\theta \rightarrow \infty$, the oscillatory part of the flow diminishes. When both $\delta \gg 1$ and $\theta \gg 1$, the flow is in the hydrodynamic or slip regimes.

Also, the dimensionless independent space and time variables $r = r'/R$, $z = z'/R$ and $t = t'\omega$, are introduced. The dimensionless area and perimeter of the tube cross section are defined by $A = A'/R^2$ and $\Gamma = \Gamma'/R$ respectively, while $\Gamma/A = 2$. The dimensionless amplitude of the oscillatory pressure gradient is

$$X = \frac{R}{P(z')} \frac{dP(z')}{dz'} = \frac{1}{P(z)} \frac{dP(z)}{dz}, \quad (13)$$

with $X \ll 1$. This assumption is typical in fully-developed flows (also in steady-state setups), in order to permit the linearization of the governing kinetic equation and it is valid for any pressure difference provided that the channel is adequately long [8,9]. For comparison purposes between the oscillatory and steady flow, the amplitude of the oscillatory pressure gradient is taken equal to the steady one ($dP/dz' = dP_S/dz'$). In this way, $X = X_S$, and the peak values of the macroscopic quantities (velocity, flow rate, shear stress, and pumping power) of the oscillatory flow can be compared with the corresponding ones of the steady flow.

All velocities (pulsatile, oscillatory and steady) are non-dimensionalized by the most probable speed ν . More specifically, Eq. (2) is divided by (νX) to yield

$$\hat{u}_{PUL}(t,r) = u_S(r) + \hat{u}(t,r) \quad (14)$$

where $u_S(r)$ is the steady flow velocity and $\hat{u}(t,r)$ is the oscillatory flow velocity, which may be written as

$$\hat{u}(t,r) = \Re[u(r)\exp(-it)] = \Re[u_A(r)\exp(i(u_P(r)-t))] = u_A(r)\cos[t-u_P(r)] \quad (15)$$

In Eq. (15) the subscripts A and P denote the amplitude and the phase of the complex oscillatory velocity $u(r)$. The mean velocities are also non-dimensionalized by the most probable speed ν and the resulting mean steady and oscillatory velocities are denoted by \bar{u}_S and $\bar{\hat{u}}(t)$ respectively.

Next, the dimensionless flow rate is defined by introducing (14) and (15) along with the equation of state $P = \rho\nu^2/2$ into Eq. (6) to obtain $\tilde{M}_{PUL}(t') = R^2PX\hat{G}_{PUL}(t)/\nu$, where $\hat{G}_{PUL}(t) = G_S + \hat{G}(t)$. Here, G_S is the well-known steady flow rate [8], $\hat{G}(t)$ is the oscillatory flow rate and they are given by

$$G_S = 4\int_0^1 u_S(r)rdr \quad \text{and} \quad \hat{G}(t) = 4\int_0^1 \hat{u}(t,r)rdr. \quad (16)$$

The oscillatory flow rate $\hat{G}(t)$ may be also written as

$$\hat{G}(t) = \Re[G\exp(-it)] = \Re[G_A\exp(i(G_P-t))] = G_A\cos(G_P-t) \quad (17)$$

where the flow rate G , as well its amplitude G_A and phase G_P , may be computed by integrating accordingly the corresponding velocity quantities. It is readily seen that the dimensionless flow rates may be connected to the dimensionless mean velocities by the following expressions: $G_S = 2\bar{u}_S$ and $\hat{G}(t) = 2\bar{\hat{u}}(t)$.

All stresses (pulsatile, oscillatory and steady) are non-dimensionalized by the reference pressure P . More specifically, Eq. (3) is divided by $(2PX)$ to yield

$$\hat{\tau}_{PUL}(t,r) = \tau_S(r) + \hat{\tau}(t,r) = \tau_S(r) + \tau_A(r)\cos[t-\tau_P(r)], \quad (18)$$

where $\tau_S(r)$ is the steady shear stress and $\hat{\tau}(t,r)$ is the oscillatory shear stress. In Eq. (18) the subscripts A and P denote the amplitude and the phase of the corresponding oscillatory complex shear stresses. The pulsatile wall shear stress is obtained for $r=1$.

All forces in Eqs. (7-9) are divided by (PX_pR^2) to yield the corresponding dimensionless ones:

$$\hat{F}_{PUL,I}(t) = \hat{F}_I(t) = dzA\frac{\delta}{\theta}\frac{d\hat{G}}{dt} = dzA\frac{\delta}{\theta}G_A\sin(G_P-t) \quad (19)$$

$$\hat{F}_{PUL,V}(t) = F_{S,V} + \hat{F}_V(t) = 2dz\Gamma[\tau_{S,W} + \hat{\tau}_W(t)] = 2dz\Gamma[\tau_{S,W} + \tau_{W,A}\cos(\tau_{W,P}-t)] \quad (20)$$

$$\hat{F}_{PUL,P}(t) = F_{S,P} + \hat{F}_P(t) = Adz(1 + \cos t) \quad (21)$$

The balance equations of the dimensionless steady $F_{S,V} = F_{S,P}$ and oscillatory $\hat{F}_I(t) + \hat{F}_V(t) = \hat{F}_P(t)$ forces are:

$$\text{Steady: } \bar{\tau}_{S,W} = 1/4 \quad (22)$$

$$\text{Oscillatory: } \frac{\delta}{\theta}G_A\sin(G_P-t) + 4\bar{\tau}_{W,A}\cos(\bar{\tau}_{W,P}-t) = \cos t \quad (23)$$

Equation (22) has been also reported in previous works related to steady fully-developed flows [10,11]. Equation

(23) is the corresponding one for oscillatory flow. The first and second terms at the left hand side refer to the inertia and viscous forces respectively, while the right hand side refers to the pressure forces.

Finally, the dimensionless pumping power is derived by dividing Eq. (12) by $(\nu X)(XP)R^2$ to find $\hat{E}_{PUL}(t) = E_S + \hat{E}(t)$, where the steady pumping power is $E_S = AdzG_S/2$ and the oscillatory one is written as

$$\hat{E}(t) = \frac{1}{2} Adz \cos t G(t) = \frac{1}{2} Adz \cos t \Re \left[G_A \exp(i(G_P - t)) \right] = \frac{1}{2} Adz G_A \cos t \cos(G_P - t) \quad (24)$$

By integrating Eq. (34) over one oscillation cycle, the average pumping power over the cycle is formed as

$$\bar{E} = \frac{1}{2\pi} \int_0^{2\pi} \hat{E}(t) dt = \frac{1}{4} Adz G_A \cos(G_P). \quad (25)$$

In the low frequency regime, where $G_P \rightarrow 0$ and $G_A \simeq G_S$, it is seen that the average oscillatory pumping power is half of the corresponding steady one ($\bar{E} \simeq E_S/2$).

The prescribed pulsatile flow is solved here in the whole range of δ and θ , which may vary from zero to infinity. The solution is based on the kinetic modeling described in the next section.

3 KINETIC FORMULATION

For arbitrary values of the parameters δ and θ the flow must be simulated based on kinetic theory, where the main unknown is the distribution function $f = f(t', \mathbf{r}', \xi)$, which is a function of time t' , position vector $\mathbf{r}' = (x', y', z')$ and molecular velocity vector $\xi = (\xi_x, \xi_y, \xi_z)$. The unknown distribution obeys the time-dependent nonlinear two-dimensional BGK equation [12]

$$\frac{\partial \tilde{f}}{\partial t'} + \xi_r \frac{\partial \tilde{f}}{\partial r'} - \frac{\xi_\varphi}{r'} \frac{\partial \tilde{f}}{\partial \varphi} + \xi_z \frac{\partial \tilde{f}}{\partial z'} = \frac{P}{\mu} (f^M - \tilde{f}) \quad (26)$$

where (P/μ) is the collision frequency and

$$f^M(t', \mathbf{r}', \xi) = n \left(\frac{m}{2\pi kT} \right)^{3/2} \exp \left[-m(\xi - \hat{U}_{PUL})^2 / (2kT) \right] \quad (27)$$

is the local Maxwellian distribution. Due to the assumption of isothermal fully-developed flow the temperature T is constant and the number density $n = n(z')$ varies only in the z' -direction. Also, the macroscopic velocity has only the z' -component and it is the same with the pulsatile velocity defined in Eq. (2), i.e., $\hat{U}_{PUL} = (0, 0, \hat{U}_{PUL})$. The pulsatile velocity $\hat{U}_{PUL}(t', r')$ and shear stress $\hat{\Pi}_{PUL}(t', r')$ (defined in Eq. (3)) at some position z' in the flow direction may be obtained by the first and second moments of f :

$$\hat{U}_{PUL}(t', r') = \frac{1}{n} \int \xi_z \tilde{f}(t', \mathbf{r}', \xi) d\xi \quad \text{and} \quad \hat{\Pi}_{PUL}(t', r') = m \int \xi_r (\xi_z - \hat{U}_{PUL}) \tilde{f}(t', \mathbf{r}', \xi) d\xi \quad (28)$$

The condition of small local pressure gradient ($X \ll 1$) allows the linearization of Eq. (26) by representing the unknown distribution function as

$$f(t', \mathbf{r}', \xi) = f_0 \left[1 + X \hat{h}_{PUL}(t, r, \mathbf{c}) + Xz \exp(-it) \right], \quad (29)$$

where $\mathbf{c} = \xi/\nu$, $f_0 = \frac{n}{\pi^{3/2} \nu^3} \exp[-c^2]$ is the absolute Maxwellian and $\hat{h}_{PUL}(t, x, y, \mathbf{c})$ is the unknown perturbed distribution function referring to the pulsatile fully-developed flow, which may be decomposed as

$$\hat{h}_{PUL}(t, r, \mathbf{c}) = h_S(r, \mathbf{c}) + \hat{h}(t, r, \mathbf{c}) \quad (30)$$

with $\hat{h}_S(r, \mathbf{c})$ and $\hat{h}(t, r, \mathbf{c})$ referring to the steady and oscillatory parts respectively. Substituting expressions (29) and (30) into Eq. (26) and introducing the dimensionless variables, yields the following two linearized BGK kinetic model equations:

$$c_r \frac{\partial h_S}{\partial r} - \frac{c_\varphi}{r} \frac{\partial h_S}{\partial \varphi} = \delta [2c_z u_S(r) - h_S(r, \mathbf{c})] \quad (31)$$

$$\frac{\delta}{\theta} \frac{\partial \hat{h}}{\partial t} + c_r \frac{\partial \hat{h}}{\partial r} - \frac{c_\varphi}{r} \frac{\partial \hat{h}}{\partial \varphi} + c_z e^{-it} = \delta [2c_z \Re \hat{u}(t, r) - \hat{h}(t, r, \mathbf{c})] \quad (32)$$

where $c_r = \zeta \cos \varphi$ and $c_\varphi = \zeta \sin \varphi$. The first one describes the steady fully-developed flow through a circular tube and it is solved in [10]. The second one describes the oscillatory fully-developed flow and it is the one to be solved in the present work. However, since it is also solved in [9], the non-dimensionalization and the linearization are omitted here and only the final kinetic equation is given as

$$\zeta \cos \varphi \frac{\partial Y}{\partial r} - \frac{\zeta \sin \varphi}{r} \frac{\partial Y}{\partial \varphi} + \left(\delta - i \frac{\delta}{\theta} \right) Y = \delta u - \frac{1}{2}. \quad (33)$$

The complex velocity and shear stress are given by the moments of Y as

$$u(r) = \frac{1}{\pi} \int_0^{2\pi} \int_0^\infty Y e^{-\zeta^2} \zeta d\zeta d\varphi \quad \text{and} \quad \tau(r) = \frac{1}{\pi} \int_0^{2\pi} \int_0^\infty (\zeta \cos \varphi) Y e^{-\zeta^2} \zeta d\zeta d\varphi. \quad (34)$$

Turning to the boundary conditions it is noted that purely diffuse scattering is assumed at the wall, i.e., $f^+ = f_w^M$, where the superscript (+) denotes particles departing from the wall and f_w^M is the Maxwellian distribution defined by the wall conditions. Based on the above and following the linearization and projection procedures in [9] it is deduced that the wall boundary ($r=1$) is given by

$$Y(1, \zeta, \varphi) = 0, \quad \pi/2 < \varphi < 3\pi/2. \quad (35)$$

At the symmetry axis ($r=0$), molecules are reflected specularly, i.e.,

$$Y(0, \zeta, \varphi) = Y(0, \zeta, \varphi - \pi), \quad 0 < \varphi < \pi/2, \quad 3\pi/2 < \varphi < 2\pi. \quad (36)$$

The kinetic formulation of the oscillatory fully-developed flow setup is properly defined by Eqs. (33-36). The numerical solution is deterministic and it has been extensively applied in steady-state and time-dependent flow configurations with considerable success [8,13,14].

4 RESULTS AND DISCUSSION

In Fig. 1 the oscillatory flow rate $\hat{G}(t) = G_A \cos(t - G_P)$ and the pulsatile one $\hat{G}_{PUL}(t) = G_S + \hat{G}(t)$ are plotted versus time $t \in [0, 2\pi]$ for $\delta = [0.1, 1, 10]$ and $\theta = [0.1, 1, 10]$. The oscillatory flow rate over one cycle, takes both positive and negative values (the fluid is moved forth and back) and the time average flow rate over one cycle is zero (no net flow). The amplitude of the oscillatory flow rate is reduced as θ is decreased and this behavior becomes even stronger as δ is increased (less gas rarefaction). The time evolution of the pulsatile flow rate is obtained by superimposing on the oscillatory flow rate the corresponding steady one, which depends only on δ . Since the steady flow is independent of θ the behavior of the pulsatile flow rate with respect to θ is qualitatively the same with the oscillatory one. Consequently, at large θ (e.g., $\theta=10$), where the amplitude of the oscillatory flow rate is large, the difference between the amplitude of the pulsatile flow rate and the corresponding steady one is also large. On the contrary, as the oscillatory flow tends to diminish, which is happening as θ is decreased and δ is increased, the pulsatile flow rate gradually tends to the steady one at the corresponding δ . This is particularly evident at $\theta=0.1$ and $\delta=10$, where $\hat{G}_{PUL}(t) \simeq G_S$. It is also noted that

the pulsatile flow rate takes only positive values, i.e., there is no flow reversal at any time. This observation may be technologically significant in applications where a pulsatile flow is desired, e.g. in order to enhance mixing or heat transfer under rarefied conditions, without however having particles moving opposite to the pumping direction or hot gas transported backwards into colder regions.

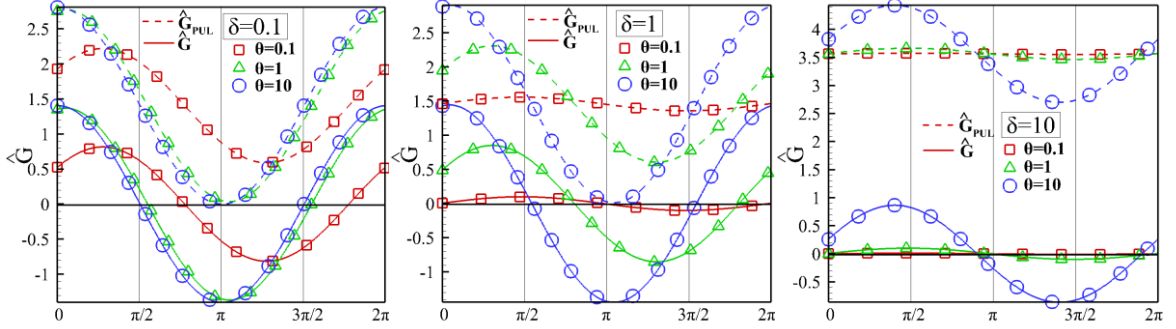


Figure 1: Oscillatory \hat{G} and pulsatile \hat{G}_{PUL} flow rates over one oscillation period for various values of δ and θ .

In Fig. 2, the oscillatory mean wall shear stress amplitude $\tau_{W,A}(\delta, \theta)$ and phase $\tau_{W,P}(\delta, \theta)$ are plotted in terms of δ with $\theta = [0.1, 1, 10, 50, 10^2]$. For very small values of δ the mean wall shear stress amplitude $\tau_{W,A}$ takes the same value as the corresponding steady one $\tau_{S,W} = 0.25$. As δ is increased it is slightly reduced and then, from some δ in the late transition or slip regimes it is rapidly decreased. The value of δ where this rapid decrease of $\tau_{W,A}$ is starting depends on θ and it is increasing as θ is decreasing. Thus, the variation of $\tau_{W,A}$ depends monotonically on δ and does not include the local maxima observed in the variation of G_A that has been reported in [9]. With regard to the phase difference, $\tau_{W,P}$ is always monotonically increased with δ and it is almost independent of the oscillation frequency θ . At very small values of δ it is almost zero, then at moderate values of δ it is rapidly increased and finally, at large values of δ it is asymptotically increased reaching the limiting value of $\pi/2$. The dependency of the oscillatory wall shear stress $\hat{\tau}_W$ on δ and θ is very close to the corresponding one of the flow rate \hat{G} shown in Fig. 1 and therefore, it is omitted here.

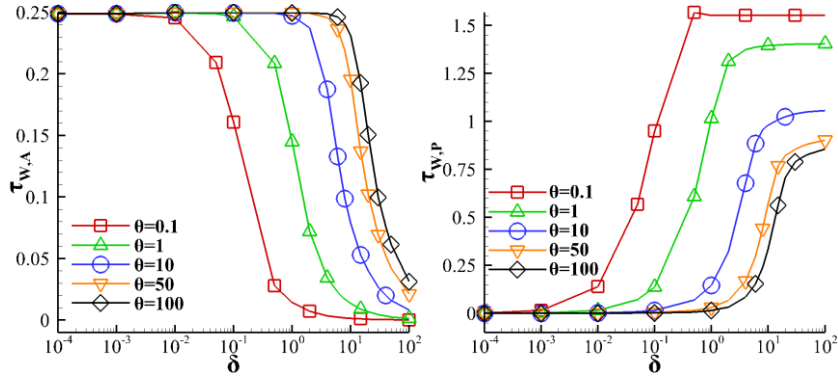


Figure 2: Oscillatory wall shear stress amplitude $\bar{\tau}_{W,A}$ and phase $\bar{\tau}_{W,P}$ in terms of δ for various values of θ .

Next in Fig. 3, the oscillatory pumping power, defined as $\hat{E}/(Adz) = G_A \cos(G_P - t) \cos t / 2$ (see Eq. (24)), is plotted in terms of $t \in [0, 2\pi]$ for $\delta = [0.1, 1, 10]$ and $\theta = [0.1, 1, 10, 10^2]$. The pumping power has two peaks within each oscillatory cycle because it consists of the product of the oscillatory pressure times the oscillatory flow. Its integral over one cycle is not zero in order to drive the oscillatory flow, although the oscillatory net flow is zero. The dependency of the oscillatory pumping power on δ and θ is similar to the one observed for the flow rate, i.e. in general, as θ is decreased (the oscillation frequency is increased) its amplitude is decreased and its phase lag is increased. This behavior becomes more dominant as δ is increased.

As pointed above, even when the flow is reversed, which is occurring at the second half of the oscillation cycle at time $t \in [\pi/2, \pi]$ where the flow rate is negative, the pumping power remains positive. It is seen however, in Fig. 3 that at certain times $t \in [0, 2\pi]$, the oscillatory pumping power may become negative. This is more evident at large δ and small θ and it is occurring because in dense gases and at relatively high frequencies the flow rate is completely out of phase with the pressure gradient (it becomes proportional to a sinusoidal function). Thus, when the pressure gradient becomes negative and the flow is reversed, the sign of the flow rate remains positive for a certain time interval and during this interval the overall pumping power becomes negative. This time interval is increased as θ is decreased. Of course in rarefied gases and/or low frequencies \hat{E} is always positive because the flow rate is in phase with the pressure gradient.

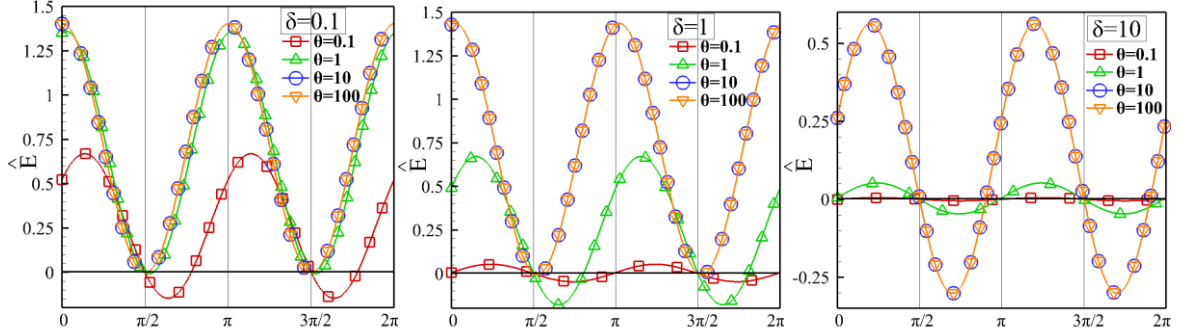


Figure 3: Oscillatory pumping power \hat{E} over one oscillation period for various values of δ and θ (pumping power is divided by Adz).

Finally, in Fig. 4, the oscillatory inertia, \hat{F}_I , viscous \hat{F}_V and pressure \hat{F}_p forces are plotted over one oscillation period $t \in [0, 2\pi]$ for $\delta = [0.1, 1, 10]$ and $\theta = [0.1, 1, 10]$. In all cases the force balance equation (23) is satisfied. The inertia forces refer to the core flow and the viscous forces refer to the Stokes layer. The phase difference between these two forces is always $\pi/2$. In the cases of $(\delta = \theta = 0.1)$, $(\delta = \theta = 1)$ and $(\delta = \theta = 10)$ the viscous and inertia forces lag and lead the corresponding pressure force respectively by a phase angle of $\pi/4$. The amplitudes of the two forces are about the same. Then, in the cases of $(\delta = 10, \theta = 1, 0.1)$ and $(\delta = 1, \theta = 0.1)$, the inertia forces almost coincide with the corresponding pressure forces, while the viscous forces lag the other two forces by almost $\pi/2$ and their amplitudes are close to zero. The flow consists of two regions: the core region oscillating in a plug mode and, adjacent to the wall, the oscillating thin viscous or Stokes layer with the velocity overshooting. In the cases of $(\delta = 1, \theta = 10)$ and $(\delta = 0.1, \theta = 1, 10)$ this behavior is reversed, i.e., the viscous coincide with pressure forces, while the inertia forces lead by almost $\pi/2$ and their amplitudes are close to zero. The flow consists of one oscillating region with no velocity overshooting. This description clarifies the behavior of the inertia and viscous forces in terms of θ and δ .

5 CONCLUDING REMARKS

The pulsatile isothermal fully-developed flow in a circular tube is investigated by decomposing the flow into the steady and oscillatory parts. The steady part is well-known and therefore, the investigation is focused mainly on the oscillatory part, which is numerically solved, based on the time-dependent linear BGK equation, in a wide range of the gas rarefaction parameter δ and the oscillation parameter θ .

Always as θ is decreased (i.e., the oscillation frequency is increased) the amplitude of all macroscopic quantities is decreased and their phase lag with respect to the pressure gradient is increased. Actually, at very small θ the amplitude tends to diminish and the phase lag approaches the limiting value of $\pi/2$. It is important to note however, that as δ is decreased (i.e., the gas becomes more rarefied) higher frequencies are needed to trigger the behavior described above. The amplitude of the oscillatory pressure gradient is taken to be equal with the steady pressure gradient. Having this in mind it is useful to note that the pulsatile flow rate is always positive and therefore, there is no flow reversal. Furthermore, the amplitude of the wall shear stress is increased with θ being always smaller than the corresponding steady ones. In terms of δ the wall shear stress amplitude remains almost constant in the free molecular and transition regimes and then it is rapidly reduced. The phase lag of the wall shear stress is increased as δ is increased.

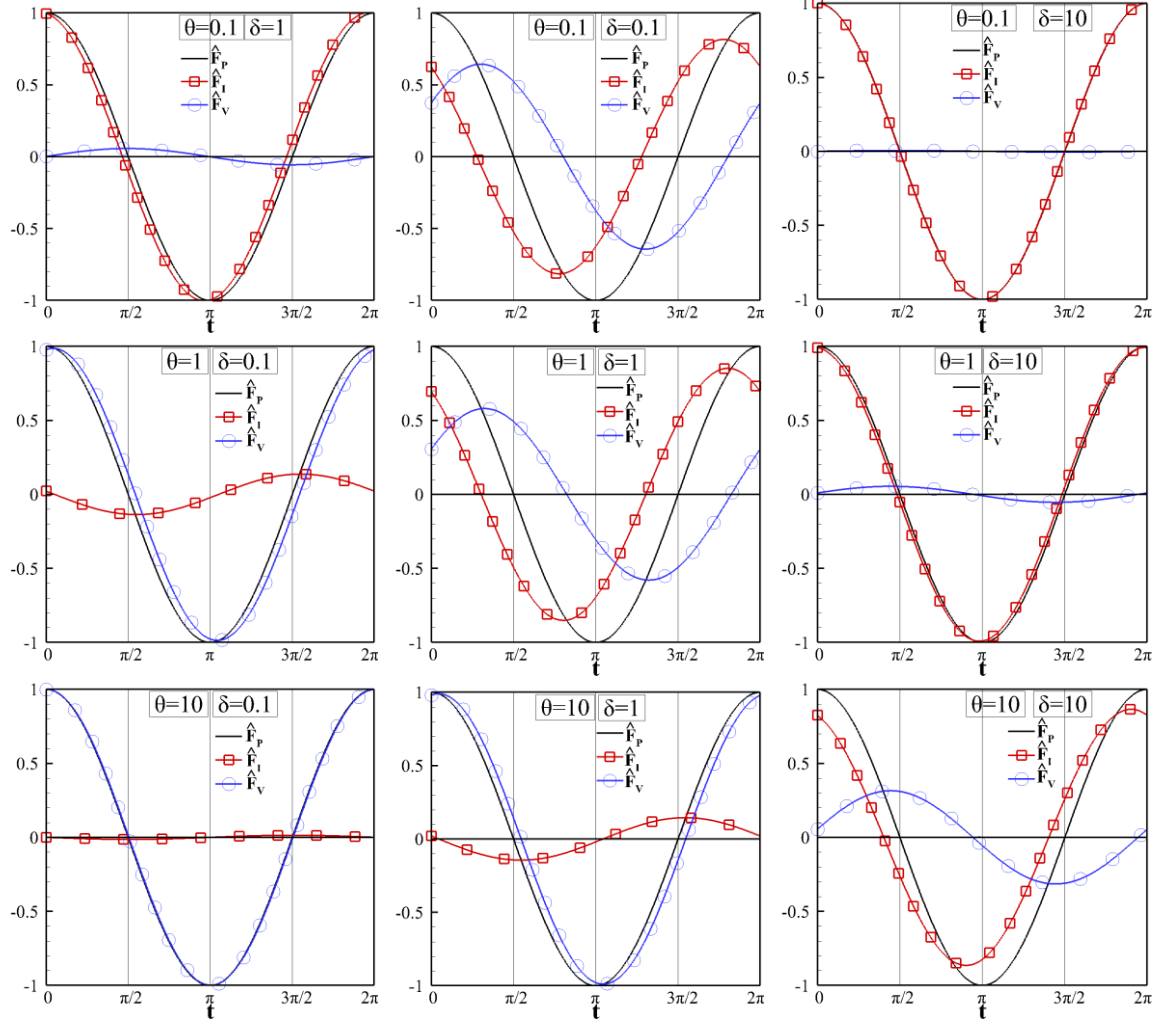


Figure 4: Oscillatory inertia \hat{F}_I , viscous \hat{F}_V and pressure \hat{F}_P forces over one oscillation period for various values of δ and θ (forces are divided by Adz).

The oscillatory pumping power has two peaks within each oscillatory cycle and its integral over one cycle is not zero. The nonzero pumping power is needed to maintain the oscillatory flow, even though the oscillatory net flow is zero and it is increased as the oscillation frequency is reduced. By adding the oscillatory pumping power to the steady one, yields the total power to maintain the pulsatile flow.

Finally, the inertia and viscous forces, having always a phase difference of $\pi/2$, are computed in a wide range of δ and θ . Their amplitudes are about the same when $\delta = \theta$. As δ is increased and θ is decreased the inertia forces dominate causing a core oscillating plug flow with a thin Stokes layer. In the opposite situation (i.e., as δ is decreased and θ is increased) the viscous forces become more important causing a typical viscous oscillatory flow without velocity overshooting.

ACKNOWLEDGEMENTS

This work has been carried out within the framework of the EUROfusion Consortium and has received funding from the Euratom research and training programme 2014-2018 under grant agreement No 633053. The views and opinions expressed herein do not necessarily reflect those of the European Commission.

REFERENCES

1. Vasileiadis, N., Tatsios, G., Misdanitis, S. and Valougeorgis, D. (2016), "Modeling of complex gas distribution systems operating under any vacuum conditions: Simulations of the ITER divertor pumping system", *Fusion Engineering and Design*, Vol. 103, pp. 125-135.
2. Abreu, R. A., Troup, A. P. and Sahm, M. K. (1994), "Causes of anomalous solid formation in the exhaust systems of low-pressure chemical vapor deposition and plasma enhanced chemical vapor deposition semiconductor processes", *Journal of Vacuum Science and technology B*, Vol. 12 (4), pp. 2763-2767.
3. Zamir, M. (2000), "*Physics of Pulsatile Flow*", Springer-Verlag, New York.
4. Blythman, R., Persoons, T., Jeffers, N., Nolan, K. P. and Murray, D. B. (2017), "Localized dynamics of laminar pulsatile flow in a rectangular channel", *International Journal of Heat and Fluid Flow*, Vol. 66, pp. 8-17.
5. Batikh, A., Caen, R., Colin, S., Baldas, L., Kourta, A. and Boisson, H. C. (2008), "Numerical and experimental study of micro synthetic jets for active flow control", *International Journal of Heat and Technology*, Vol. 26 (1), pp. 139-145.
6. Wang, S., Baldas, L., Colin, S., Kourta, A. and Mazellier, N. (2014), "Numerical and experimental characterization of a micro-oscillator for flow control", Proceedings of the 4th European Conference on Microfluidics, Limerick, Ireland, 10-12 December 2014.
7. Colin, S., Aubert, C. and Caen, R. (1998), "Unsteady gaseous flows in rectangular microchannels: frequency response of one or two pneumatic lines connected in series", *European Journal of Mechanics B/Fluids*, Vol. 17, pp. 79-104.
8. Sharipov, F. (2016), "*Rarefied Gas Dynamics. Fundamentals for Research and Practice*", Wiley-VCH, New Jersey.
9. Tsimpoukis, A. and Valougeorgis, D. (2018), "Rarefied isothermal gas flow in a long circular tube due to oscillating pressure gradient", *Microfluidics and Nanofluidics*, Vol. 22, 5.
10. Varoutis, S., Lihnaropoulos, J., Mathioulakis, D., Tserepi, A. and Valougeorgis, D. (2008), "Estimation of the Poiseuille number and of the exact hydraulic diameter in rarefied gas flows through channels of various cross sections", *1st European Conference on Microfluidics (mFlu'08)*, Bologna, Italy, 10-12 December 2008.
11. Naris, S. and Valougeorgis, D. (2008), "Rarefied gas flow in a triangular duct based on a boundary fitted lattice", *European Journal of Mechanics B/Fluids*, Vol. 27, pp. 810-822.
12. Bhatnagar, P. L., Gross, E. P. and Krook, M. A. (1954), "A model for collision processes in gases", *Physical Review*, Vol. 94, pp. 511-525.
13. Lihnaropoulos, J. and Valougeorgis, D. (2011), "Unsteady vacuum gas flow in cylindrical tubes", *Fusion Engineering and Design*, Vol. 86, pp. 2139-2142.
14. Buchina, O. and Valougeorgis, D. (2012), "Oscillatory heating in a microchannel at arbitrary oscillation frequency in the whole range of the Knudsen number", *Journal of Physics: Conference Series* 362, 012015.